Available online at www.sciencedirect.com
ScienceDirect
Journal of the European Ceramic Society 27 (2007) 3345–3349
www.elsevier.com/locate/jeurceramsoc

Temperature dependence of mechanical properties of alumina up to the onset of creep

Estíbaliz Sánchez-González [a], Pedro Miranda [b], Juan J. Meléndez-Martínez [a], Fernando Guiberteau [b], Antonia Pajares [a,*]

[a] *Departamento de Física, Facultad de Ciencias, Universidad de Extremadura, 06071 Badajoz, Spain*
[b] *Departamento de Ingeniería Mecánica, Energética y de los Materiales, Escuela de Ingenierías Industriales, Universidad de Extremadura, 06071 Badajoz, Spain*

Available online 25 April 2007

Abstract

Mechanical properties of a commercial polycrystalline alumina are evaluated as a function of temperature up to the onset of creep. Hertzian indentation tests in combination with finite element modelling (FEM) are used to determine its elastic and plastic properties from the corresponding indentation stress–strain curves at prescribed temperatures up to 1200 °C. The results reveal a strong decline in the Young's modulus and the yield stress of the material at about 600 °C that is attributed to grain boundary degradation occurring around that temperature. The results are compared with dynamic Young's modulus and Vickers hardness measurements from the literature. The practical interest of measuring the mechanical properties of ceramics at intermediate temperatures is discussed and a general guideline to retain optimum elastic and plastic properties at intermediate temperatures is outlined.

Keywords: Mechanical properties; Al_2O_3; Hertzian test

1. Introduction

Alumina is the most important technical oxide ceramic and is widely used as a sealing element, filter, implant material, electrical and thermal insulator, wear and corrosion protection barrier, etc. Densely sintered alumina is characterised by outstanding values of strength, hardness, and wear resistance, making it especially suitable for mechanical applications. Usually, these properties are measured for quality control purposes at room temperature, while in practical applications the material has to withstand elevated temperatures. Such temperatures can affect the mechanical properties of the material, compromising its performance during service. Accordingly, the interest of analyzing the mechanical properties of alumina above room temperature is evident.

There are some results concerning the mechanical properties of alumina at high temperature in the literature. Unfortunately, most of them deal with creep behaviour, and, in spite of its practical relevance, in the intermediate temperature range the scarce data available is limited to determinations of either hardness (from Vickers indentation test)[1,2] or dynamic modulus (based on measurements of the propagation of mechanical waves in solids).[3–5]

The objective of this work was to use a recently developed method[6] based on the combination of Hertzian indentation tests with finite element modelling (FEM) to evaluate the mechanical properties of alumina from room temperature up to the onset of creep. Typical indentation stress–strain curves are obtained from the Hertzian tests, and Young's modulus, E, is calculated from the slope of the linear part of the curves by using Hertzian theory. Yield stress, Y, and strain-hardening parameter, n, are evaluated by fitting FEM results to the experimental curves. The results that were obtained with this method revealed a decrease of Young's modulus and yield stress with increasing temperature, while the strain hardening parameter stayed approximately constant over the whole temperature range that was studied. Furthermore, at about 600 °C a faster decline in the Young's modulus and a drop in the yield stress were observed, which we attributed to a grain boundary degradation occurring at that temperature.

* Corresponding author.
E-mail address: apajares@unex.es (A. Pajares).

0955-2219/$ – see front matter © 2007 Elsevier Ltd. All rights reserved.
doi:10.1016/j.jeurceramsoc.2007.02.191

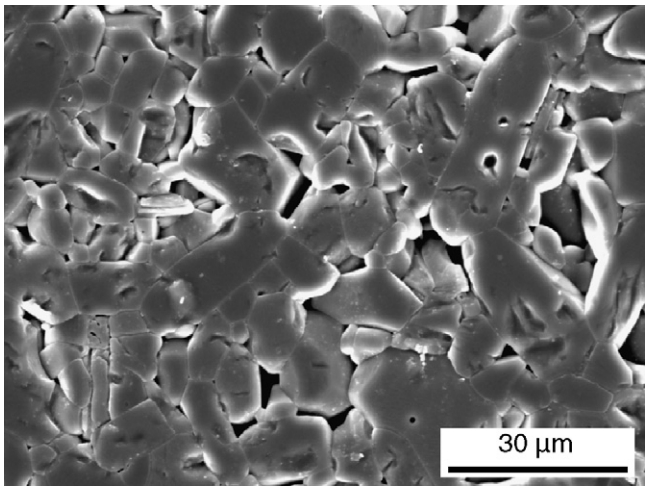

Fig. 1. SEM micrograph of polished surface of the polycrystalline alumina studied in this work after thermal etching for 1.5 h at 1500 °C.

2. Material and experimental method

The material chosen for this study was commercial polycrystalline alumina (98% dense) supplied by Goodfellow (Cambridge, UK). Plates of 2 cm × 2 cm × 0.8 cm were cut from the as-received blocks and polished with diamond paste to 1 μm finish. As can be appreciated in the SEM micrograph of Fig. 1, the material has a coarse-grained microstructure with the presence of residual porosity and extensive chipping. Alumina polished half-spheres of 3 and 9 mm radius from the same supplier were used as indenters.

3. Indentation tests

Hertzian contact tests were used to obtain the indentation stress–strain curves for alumina at several temperatures. The Hertzian tests were performed using a universal testing machine (Shimadzu model AG-IS 100 kN) at a fixed crosshead speed of 0.05 mm/min. A vertical split furnace was coupled to the testing machine to perform the test above room temperature. The half-sphere indenter and the specimen were respectively bonded to two refrigerated alumina push rods using alumina paste (ceramabond 569, Aremco Products, INC, New York). The bottom push rod holder is placed on an X–Y table to allow several tests (15–20) to be performed per sample at the selected temperature. The experimental set-up is shown in Fig. 2.

Sequences of contacts at peak loads up to 5000 N were made in air at temperatures in the range 25–1200 °C. Above 1200 °C, creep was observed in the alumina, and therefore the results are not included here. The heating ramp up to the desired test temperature was set at 6 °C/min. Before starting the contact test sequence, the system was held 1 h at the selected temperature to ensure thermal stabilization.

Before bonding the specimen to the rod, it was coated with a metallic film of about 50 nm thickness using a conventional Sputter Coater (Polaron SC7640, UK) to produce a residual impression of the contact at peak load under elastic conditions. The appropriate metal (Au, Rh–Pd, or Pt) depends on the testing

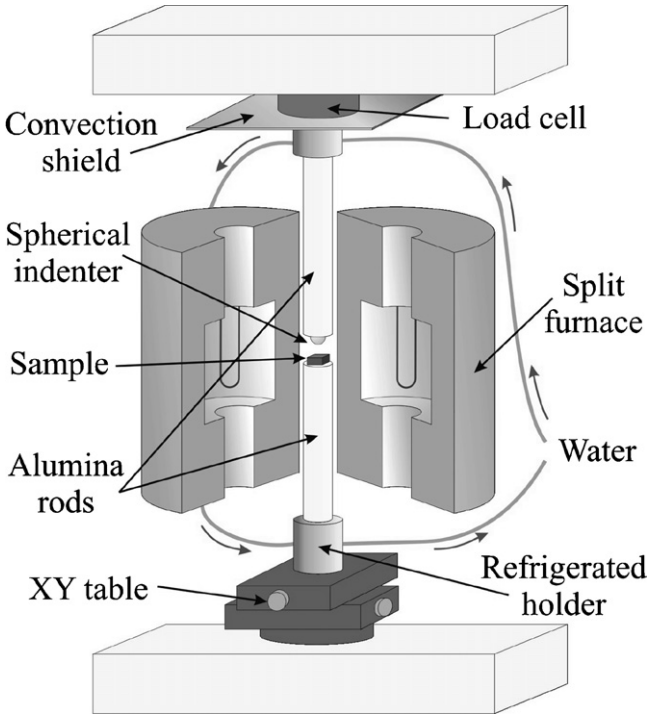

Fig. 2. Diagram of the experimental set-up used for the Hertzian tests at intermediate temperatures.

temperature, as has been discussed elsewhere.[6] Contact radius, *a,* for each peak load, *P,* and indenter radii, *r,* were measured after each test sequence using an optical microscope to obtain plots of indentation stress ($P/\pi a^2$) versus indentation strain (a/r) for each temperature.

Young's modulus E for each prescribed temperature was determined from the slope of the linear region of the indentation stress–strain curve by using the Hertzian relationship corresponding to purely elastic contacts:

$$E = \frac{3\pi\mu}{2}(1 - \nu^2) \quad (1)$$

valid for contact between like materials, where μ is the slope of that linear part of the curve and ν is the Poisson's ratio, here assumed constant and equal to 0.22.

Both the Young's modulus and Poisson's ratio are used as input parameters for the finite element modelling (FEM) described below.

4. Finite element modelling

FEM is used to determine yield properties of the alumina using ABAQUS/Standard software (Hibbitt, Karlsson & Sorensen, Inc., Pawtucket, RI). The algorithm has been described in detail elsewhere,[7] so only relevant details will be included here. The algorithm models an alumina half-sphere of 3 mm radius in axisymmetric contact with an alumina flat specimen of 15 mm thickness and 15 mm radius and incrementally loaded to a peak load of 5000 N. The specimen and sphere grids consist respectively of 11,628 and 8273 linear axisymmetric quadrilateral elements with reduced integration of

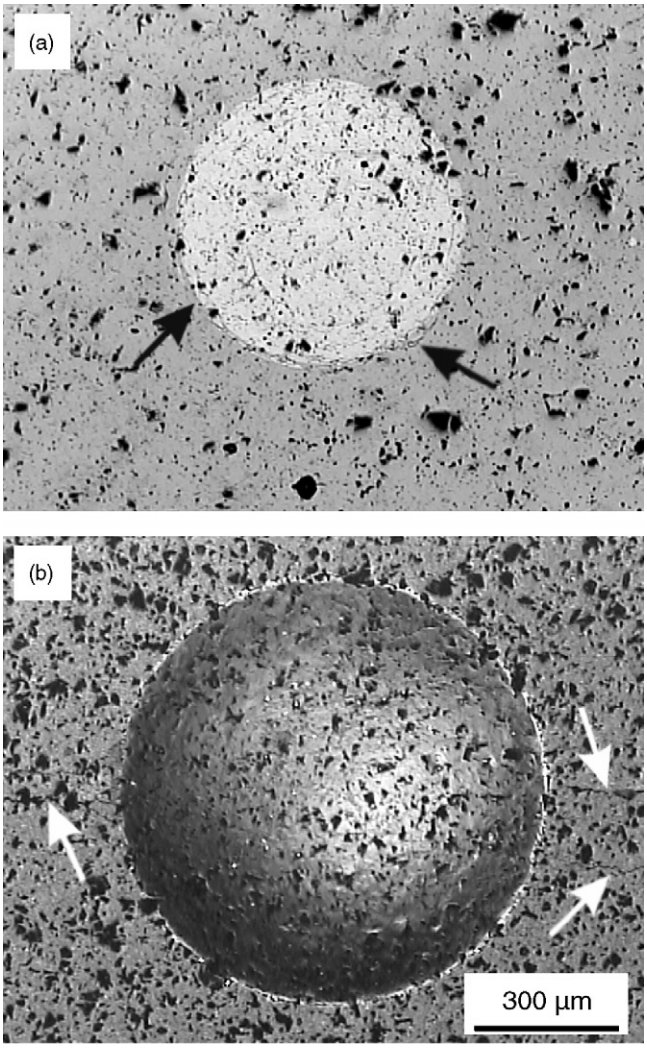

Fig. 3. Optical micrographs showing surface Hertzian damage in polycrystalline alumina generated with a polycrystalline alumina indenter of 3 mm radius at 2000 N peak load for (a) room temperature and (b) 1000 °C. Arrows indicate ring cracking in (a) and radial cracking in (b).

1 μm × 1 μm minimum dimensions. The following constitutive uniaxial elastic–plastic model is assumed for the calculations:

$$\sigma = E\varepsilon \quad (\sigma < Y), \qquad \sigma = K\varepsilon^n \quad (\sigma > Y) \tag{2}$$

where the K parameter is set to

$$K = \left(\frac{E}{Y}\right)^n Y \tag{3}$$

to guarantee the continuity of the function at $\sigma = Y$, and n is the dimensionless strain-hardening coefficient, with value between 0 (fully plastic) and 1 (fully elastic). For each temperature the two parameters, Y and n, are iteratively adjusted by trial and error to fit the indentation stress–strain data using the FEM algorithm.

5. Results

Fig. 3 shows micrographs of the surface damage induced with a 3 mm indenter radius and 2000 N load at room temperature and 1000 °C. In both cases extensive chipping is observed after grinding and polishing routines, as is expected for porous coarse-grained alumina. The residual impression is markedly more pronounced at the higher temperature. Accordingly, the corresponding contact pressure changes from 6.0 GPa at room temperature to 3.1 GPa at 1000 °C. In addition, radial cracks develop at the higher temperature due to the larger accumulation of quasi-plastic damage under the contact.

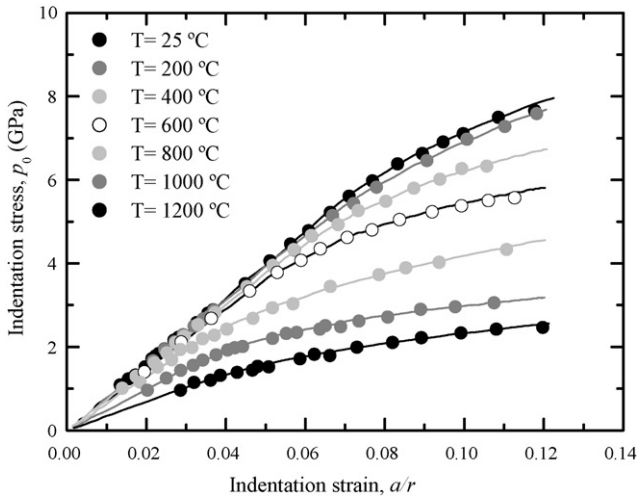

Fig. 4. Indentation stress–strain data for polycrystalline alumina at designated temperatures. Hertzian tests were performed with polycrystalline alumina indenters of 3 and 9 mm radius (not distinguished) and peak loads up to 5000 N. Solid curves through experimental data are FEM best fits.

Indentation stress–strain curves for alumina at temperatures ranging from 25 to 1200 °C are shown in Fig. 4. Each point in these curves represents a single indentation performed at a prescribed indenter radius and peak load. The solid curves through the experimental data are FEM best-fits obtained as described in the previous section. For each temperature, the initial part of the corresponding curve is linear; and, at a certain indentation stress ($p_y \approx 1.1Y$), the data depart from linearity indicating the onset of yield. Comparison of these curves clearly shows how the slope of the linear part and the yield stress decrease with temperature.

Young's modulus obtained from the slope best fit to the linear region of the stress–strain curves using Eq. (1) are plotted versus temperature in Fig. 5. At the lower temperatures the linear region is broad, and the slope and consequently Young's modulus are estimated with an uncertainty of below 2%. However, at the higher temperatures, the deviation from linearity takes place at much lower stresses and a smaller number of points are included in the calculation. Therefore the error bars corresponding to these temperatures are comparatively larger as can be seen in the figure. The solid line through the data points is an empirical fit. The results show that Young's modulus decreases slowly with increasing temperature up to 600 °C, but above that temperature the decrease is faster. Similar changes in the Young's modulus temperature dependence have been reported in the literature[3,4] but with different transition temperatures (950 and 450 °C). Fig. 5 also includes the results obtained in those works using dynamic techniques.

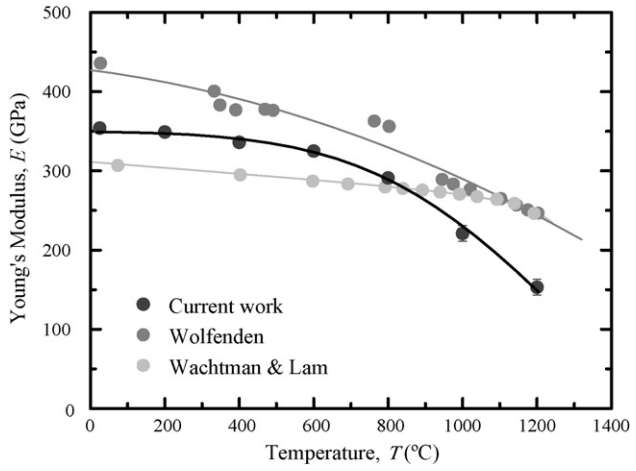

Fig. 5. Plot of Young's modulus vs. temperature for polycrystalline alumina. The data points were obtained from the slope of the linear part of the stress–strain curves of Fig. 4 and Eq. (1). Solid lines through the data are empirical fits. Also included in the figure are data for polycrystalline alumina from Wachtman & Lam and Wolfenden.[3,4]

Fig. 6 shows the yield stress determined from FEM as a function of temperature, with the error bars indicating estimated maximum uncertainties in the calculations. Solid lines through the data are empirical fits. The yield stress decreases linearly with increasing temperature up to about 600 °C. Then an abrupt drop is observed, and after that the yield stress continues its linear decline but at a lower rate (1.7 MPa/°C compared to 3.0 MPa/°C before the drop). Also included in this figure are results for Vickers hardness obtained by other authors[1,2] showing a linear decrease in hardness of alumina over the whole temperature range.

The strain hardening of the material was also obtained from FEM. It was approximately constant over the whole temperature range and equal to 0.1, indicating a very reduced or negligible strain-hardening capability in this material.

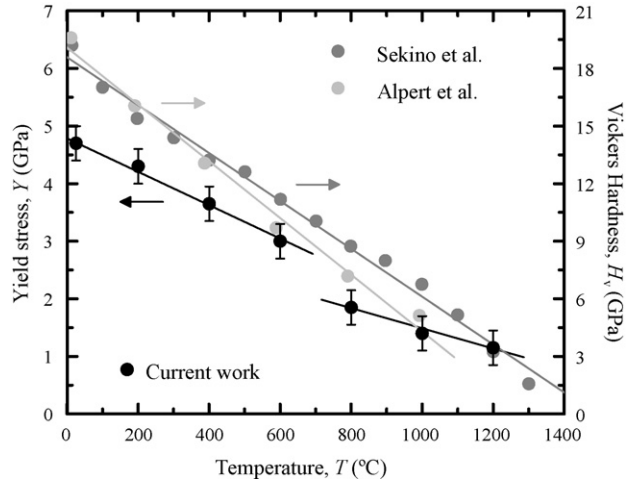

Fig. 6. Plot of yield stress from this work and Vickers hardness from Sekino et al. and Alpert et al.[1,2] vs. temperature for polycrystalline alumina. For each temperature, yield stress has been iteratively adjusted by trial and error to fit the indentation stress–strain data using the FEM algorithm. Solid lines through the data are empirical fits. Note the hardness scale (right) has been selected to be three times that of the yield stress (left) to match the empirical relation $H = 3Y$.

6. Discussion

In this work, we have used a simple mechanical test, Hertzian indentation, in combination with FEM, to determine the indentation stress–strain curves, as well as to measure Young's modulus, yield stress and strain hardening parameter of a commercial polycrystalline alumina from room temperature to 1200 °C. Although, the advantages of this methodology have been discussed in detail elsewhere,[6] we would like to highlight its effectiveness in investigating mechanical properties of ceramics at intermediate-to-high temperatures. To the best of our knowledge, it is the only method able to simultaneously provide elastic and plastic properties without relying on sophisticated electronic equipment, which are expensive and subject to thermal drift and analogous problems.

Simple micrographic examination of the testing surface (Fig. 3) qualitatively reveals the major effect of temperature in the deformation of alumina under contact stresses. In good agreement with the microscopic observations, the indentation stress–strain curves of Fig. 4 indicate a decrease in Young's modulus and yield stress with temperature.

The room temperature value of Young's modulus for polycrystalline alumina (354 ± 2 GPa) and its reduction with temperature are consistent with data found in the literature (see Fig. 5). Undoubtedly, the differences between the three sets of data in Fig. 5 is most likely associated with dissimilar microstructures in the materials tested in each work (related to differences in the starting powders, processing routes, etc.). In the alumina studied in this work, the Young's modulus slowly decreased with temperature up to about 600 °C, decreasing more sharply above this temperature. As has been suggested in the literature,[3,8] the rapid decrease of Young's modulus at the higher temperatures is caused by grain boundary sliding, and not by changes in the properties of individual grains. Obviously, the temperature at which grain-boundary sliding begins to govern Young's modulus behaviour will again depend on the specific microstructure of the material studied.

The yield stress decreases with increasing temperature, which is consistent with the Vickers hardness trend observed by other authors (see Fig. 6). In the case of the Vickers test, the highly localized nature of the loading results in multiple slip system dislocation activity, even at room temperature, as has been shown in alumina by transmission electron microscopy.[9] Accordingly, the strong temperature dependence of Vickers hardness has been explained on the basis of thermally activated mechanisms that involve dislocations.[1] In the case of the Hertzian test, this explanation is not plausible because the contact pressure at the yield point corresponding to room temperature (about 5 GPa) is well below the contact pressure induced in the Vickers tests (about 20 GPa), and consequently the shear stresses are not high enough to activate dislocation movement. Instead, as has been reported in the literature, intergranular microcracking is the damage mode activated in alumina under contact stresses at room temperature.[10,11] These microcracks are preceded by intragrain twining, and nucleate at the intersection of the twin bands and grain boundaries. This damage, usually named quasiplasticity, initiates and accumulates in a region of high hydrostatic

compression and shear stress below the contact surface, and is responsible for the low yield stress values observed. Increasing the temperature presumably facilitates twining activation within the grains. Consequently, at a certain indentation load, the stresses at the grain boundary due to twin accumulation are higher than those developed in tests performed at lower temperatures. Therefore, the minimal applied stress to induce deformation by grain boundary microcracking should diminish with temperature, explaining the decrease of yield stress over the whole temperature range (Fig. 6).

The abrupt drop of the yield stress values which takes place above 600 °C must be related to a degradation of the grain boundaries at this temperature, which reduces the stress necessary to nucleate intergranular microcracks. Notice that, as already mentioned, Young's modulus decreases more sharply above 600 °C due to grain boundary sliding, which also suggests possible deleterious changes in the grain boundaries at this temperature. Moreover, results reported by Lankford[12] in Lucalox alumina have shown that, while at 23 °C the cracking around Vickers indentations is transgranular, at 1000 °C it is intergranular, also suggesting a degradation of grain boundary strength at high temperature.

Our results have some interesting implications. In particular, they show that in polycrystalline ceramics the grain boundaries play a crucial role in the Young's modulus and yield stress values at intermediate temperatures. To retain the relatively high stiffness and hardness of ceramics at intermediate temperatures, processing routes aimed at introducing strong grain boundaries are necessary. However, it should be taken into account that strong grain boundaries negatively affect toughness. Indeed, it is well known that one of the routes to increase the room temperature toughness of ceramics is to introduce weak grain boundaries, since weak interfaces enhance the crack-bridging mechanism. Accordingly, the toughness of the alumina studied in this work should be higher above 600 °C. The fact that no cone cracking is observed in Fig. 2b (compare Fig. 2a) seems to support this, although it needs to be further verified by other means.

Acknowledgements

This work was funded by the Ministerio de Ciencia y Tecnología (Government of Spain) and the Fondo Social Europeo through grant MAT2003-05584.

References

1. Alpert, C. P., Chan, H. M., Bennison, S. J. and Lawn, B. R., Temperature-dependence of hardness of alumina-based ceramics. *J. Am. Ceram. Soc.*, 1988, **71**, C371–C373.
2. Sekino, T., Nakajima, T., Ueda, S. and Niihara, K., Reduction and sintering of a nickel-dispersed-alumina composite and its properties. *J. Am. Ceram. Soc.*, 1997, **80**, 1139–1148.
3. Wachtman, J. B. and Lam, D. G., Young modulus of various refractory materials as a function of temperature. *J. Am. Ceram. Soc.*, 1959, **42**, 254–260.
4. Wolfenden, A., Measurement and analysis of elastic and anelastic properties of alumina and silicon carbide. *J. Mater. Sci.*, 1997, **32**, 2275–2282.
5. Fukuhara, M. and Yamauchi, I., Temperature-dependence of the elastic-moduli, dilational and shear internal frictions and acoustic-wave velocity for alumina, (Y)TZP and beta'-sialon ceramics. *J. Mater. Sci.*, 1993, **28**, 4681–4688.
6. Sanchez-Gonzalez, E., Miranda, P., Melendez-Martinez, J. J., Guiberteau, F. and Pajares, A., Application of Hertzian tests to investigate mechanical properties of ceramics at intermediate temperatures. *J. Am. Ceram. Soc.*, 2007, **90**, 149–153.
7. Miranda, P., Pajares, A., Guiberteau, F., Deng, Y. and Lawn, B. R., Designing damage-resistant brittle-coating structures: I bilayers. *Acta Mater.*, 2003, **51**, 4347–4356.
8. Coble, R. L. and Kingery, W. D., Effect of porosity on physical properties of sintered alumina. *J. Am. Ceram. Soc.*, 1956, **39**, 377–385.
9. Hockey, B. J., Plastic deformation of aluminum oxide by indentation and abrasion. *J. Am. Ceram. Soc.*, 1971, **54**, 223–231.
10. Guiberteau, F., Padture, N. P., Cai, H. and Lawn, B. R., Indentation fatigue—a simple cyclic Hertzian test for measuring damage accumulation in polycrystalline ceramics. *Philos. Mag. A-Phys. Condens. Matter Struct. Defect Mech. Prop.*, 1993, **68**, 1003–1016.
11. Lawn, B. R., Padture, N. P., Guiberteau, F. and Cai, H., A model for microcrack initiation and propagation beneath Hertzian contacts in polycrystalline ceramics. *Acta Metall. Mater.*, 1994, **42**, 1683–1693.
12. Lankford, J., Comparative-study of the temperature-dependence of hardness and compressive strength in ceramics. *J. Mater. Sci.*, 1983, **18**, 1666–1674.